Journal of Materials Chemistry B

ROYAL SOCIETY OF CHEMISTRY

PAPER

View Article Online
View Journal | View Issue

Check for updates

Cite this: J. Mater. Chem. B, 2024, 12, 4004

Unveiling the synergy: a combined experimental and theoretical study of β-cyclodextrin with melatonin†

Riccardo Ferrero,‡ Stefano Pantaleone, ‡ Cecilia Irene Gho, § Gjylije Hoti, Francesco Trotta, Valentina Brunella* and Marta Corno *

Received 24th November 2023,
Accepted 21st March 2024

DOI: 10.1039/d3tb02795c

rsc.li/materials-b

Melatonin (MT) is a vital hormone controlling biorhythms, and optimizing its release in the human body is crucial. To address MT's unfavorable pharmacokinetics, we explored the inclusion complexes of MT with β-cyclodextrin (β-CD). Nano spray drying was applied to efficiently synthesize these complexes in three molar ratios (MT : β-CD = 1 : 1, 2 : 1, and 1 : 2), reducing reagent use and expediting inclusion. The complex powders were characterized through thermal analyses (TGA and DSC), Fourier transform infrared spectroscopy (FTIR), and *in vitro* MT release measurements *via* high-performance liquid chromatography (HPLC). In parallel, computational studies were conducted, examining the stability of MT : β-CD complexes by means of unbiased semi-empirical conformational searches refined by DFT, which produced a distribution of MT : β-CD binding enthalpies. Computational findings highlighted that these complexes are stabilized by specific hydrogen bonds and non-specific dispersive forces, with stronger binding in the 1 : 1 complex, which was corroborated by *in vitro* release data. Furthermore, the alignment between simulated and experimental FTIR spectra demonstrated the quality of both the structural model and computational methodology, which was crucial to enhance our comprehension of optimizing MT's release for therapeutic applications.

1. Introduction

Melatonin (*N*-acetyl-5-methoxytryptamine) is an endogenous neurohormone[1] directly involved in the regulation of the sleep-wake cycle and is used for the treatment of sleep disorders, such as insomnia and decompensations caused by jet lag.[2–4] Other benefits also extend to immunomodulatory and antioxidant effects and it seems to be able to prevent aging.[5,6] Melatonin (MT) activities in therapeutic applications for cardiovascular and cardiac diseases are still under investigation,[7,8] while it is confirmed that its usage as a potential therapeutic agent promotes neurogenesis and neuron survival in neurodegenerative diseases.[9]

Owing to its pharmacokinetic features, MT has been extensively studied for application in drug delivery systems (DDSs) to improve its low water solubility and sensitivity to light.[10–13] The most versatile way is represented by the encapsulation of the drug within a suitable chemical partner that provides its protection and improves its safety profile. Host–guest complexes are indeed one of the most efficient applications to modulate the properties of a molecule through its controlled delivery and protective action. For these reasons, they play a crucial role in different fields of investigation, starting with chemistry and biology up to their pharmaceutical and medical applications.[14–16] The alternative strategy that can be more advantageous encompasses the inclusion of MT in macrocyclic host molecules such as cyclodextrins (CDs) to evoke changes in the physicochemical properties of MT as a guest molecule. In the present work, inclusion complexes of MT with CDs were studied based on previous works on this DDS.[17–19]

Cyclodextrins constitute a class of cyclic oligosaccharides composed of α-D-glucopyranose units, which present the important feature of establishing supramolecular complexes.[20] CDs possess a unique structure characterized by a hydrophilic outer surface and a hydrophobic cavity that gives these molecules a typical truncated hollow cone shape. The most commonly used CDs are composed of 6, 7 or 8 α-D-glucopyranose, linked by α-1,4 glycosidic bonds, and the Greek letter in their nomenclature indicates the number of monomeric units: α-, β-, and γ-CD corresponding to cyclodextrins with 6, 7 and 8 α-D-glucopyranose

Dipartimento di Chimica and Nanostructured Interfaces and Surfaces (NIS) Centre, Università degli Studi di Torino, Via P. Giuria 7, 10125 Torino, Italy.
E-mail: valentina.brunella@unito.it, marta.corno@unito.it

† Electronic supplementary information (ESI) available. See DOI: https://doi.org/10.1039/d3tb02795c

‡ The authors equally contributed.

§ Present address: Dipartimento di Scienza Applicata e Tecnologia, Politecnico di Torino, C.so Duca degli Abruzzi 24, 10129 Torino, Italy.

units, respectively.[21] The molecular dimensions of the CD cavities make them ideal hosts for the inclusion complex formation with diverse molecules; as an example, α-CD (with a cavity diameter of 4.7–5.3 Å) can form inclusion complexes with small organic molecules or characterized by aliphatic side chains, while β-CD (cavity diameter of 6.0–6.5 Å) is the suitable host for organic molecules such as aromatic or heterocyclic rings. γ-CD (cavity diameter of 7.5–8.3 Å) is the largest of the mentioned cyclodextrins and encapsulates properly macrocycles and steroids.[20,22–24]

In recent years, depending on the needful application, a variety of methods were exploited to prepare β-CD and drug inclusion complexes: treatments by mixing solutions of β-CD and MT opened the way to form the corresponding complex, up to procedures without solvents (kneading method), co-evaporation and lyophilization.[25] The kneading method permits a very low amount of the solvent to be employed but requires a perfect balance of the reagents. On the other hand, lyophilization involves a process in which solvent is removed in vacuum after cooling but it is more expensive than conventional drying.[26]

In this article, we propose an efficient approach to achieve the inclusion complex using the spray drying technique, which consists of introducing a feed solution into an atomizer to produce small droplets of the solution exposed to high air temperatures.[27] Feed solutions are made up in the aqueous environment, from which water evaporates rapidly so that the encapsulation process occurs. The resulting samples are powders characterized by a low amount of moisture and nanometric-size particles.[28] Nano Spray Dryer synthetic pathway provides high production rates and low operating costs: for these reasons, it is considered a commercially applicable drying method in Drug Delivery Systems.[29] Current applications of Nano Spray Dryer concern encapsulation of organic molecules through a host–guest interaction[30–32] also in combination with a cyclodextrin forced to interact with essential oils[33] or levocetirizine.[34]

Computational chemistry is a well-established and paradigmatic pillar in the study of drug delivery systems.[35,36] The continuous growth of computational power has also made it possible to study large systems at accurate DFT levels, thus allowing the comprehension of the complexation/release mechanism of a certain drug and its delivery system at an atomistic level. This knowledge is fundamental to optimizing the DDS itself, making it more effective, greener, and more efficient. On the topic of CD inclusion complexes several computational works have been performed in the last few years.[37–39] Stachowicz *et al.* studied the different conformations of β-CD in the gas phase at the B3LYP level, featuring the possible H-bond patterns generated by the hydroxymethyl groups of the different glucopyranose units.[40] To investigate the structures of the three most used CDs (α, β and γ), some of us have recently applied the r^{2}SCAN-3c composite functional obtaining a complete benchmark.[41]

Previous studies have focused on the host–guest interactions established between a drug and a CD with the employment of combined DFT methodology and experimental techniques, that corroborate the importance of the deep synergy between the theory and experiment. For example, the interactions between β-CD and *N*-methylcarbamates,[42] neochlorogenic and chlorogenic acids,[43] piroxicam,[44] olsalazine,[45] permethrin[46] and proline[47] have been studied employing infrared, Raman[46] and UV-Vis spectroscopies,[42,45,47] X-ray diffraction,[43] circular dichroism[42] and scanning electron microscopy,[44] always combined with a computational counterpart, shedding light on the complexation mechanism, on the diverse host–guest conformations, and on the assignment of the bands in the different spectroscopies. Many computational standalone works provide results on the HOMO–LUMO orbitals and how they are modified by the complexation phenomenon, the binding energies of the host–guest system and structural information such as the hydrogen bonds distribution either of the CD alone or of the inclusion complex.[48–53] DFT calculations were also performed on systems involving other CDs, in particular, α- and γ-CDs with their suitable guest partners,[54–58] according to the size of the drug and the hole of the CD. Another strategy to further optimize the complexation/release mechanism of these systems is also to model various derivatized types of CDs,[59–61] by substituting –OH moieties with –OR chains.

Due to the flexibility of CDs, semi-empirical and force field methods have also been adopted to reduce the computational cost for a proper description of all the possible conformers upon complexation.[62–64] For this reason, an equally valid approach involves molecular mechanics-based molecular dynamics (MM/MD),[65–67] which are applied to confirm experimental insights in terms of complexation affinity,[68–70] structural features[71,72] and spectroscopic analysis.[73] Different studies simulated the encapsulation of a guest with several cyclodextrins in various stoichiometric ratios,[74–78] allowing not only conformational investigations but also the study of the system evolution over time.[79–82]

Among the others, the recently developed GFN2-xTB method was shown to be almost as accurate as DFT[83,84] with the cheap computational cost typical of other semi-empirical methods (3–5 orders of magnitude lower than DFT) and successfully applied to host–guest phenomena.[85–88] A recent paper published by some of us confirmed the accuracy of the GFN2-xTB method with respect to different DFT functionals on selected melatonin/cyclodextrin complexes.[89] Therefore, starting from those results, we have largely expanded that work by means of the CREST submodule implemented in the xTB program.[90] CREST allows us to explore the potential energy surface as was recently shown with transition metal complexes,[91] as well as for the host-ligand conformations between cucurbituril and a set of medium-sized organic molecules.[92] The idea is, therefore, to combine the possibility of exhaustively exploring the conformational space of the system with cheap methods (either classical and semi-empirical), thus generating a large set of structures, whose geometries and energies are then refined at the DFT level, configuring as an approach already tested on the cyclodextrin bare system.[41]

In the present study, we have performed a combined experimental and computational investigation on the inclusion complex MT : β-CD, in which three potential molar ratios of MT : β-CD were explored (1 : 1, 2 : 1 and 1 : 2) to study all the possible complexation reactions. The complexation reaction

was achieved using the Nano Spray Dryer technique and the samples were characterized by thermal analyses (thermogravimetry and differential scanning calorimetry) and FTIR spectroscopy. Furthermore, the *in vitro* release study of the MT was performed to roughly evaluate the strength of the host–guest interaction and to provide the quantity of MT left free over time. Models of these three complexes were designed and, after conformational research performed with xTB-CREST, the low-lying energy structures were reoptimized at the DFT level and vibrational frequencies were computed to simulate the corresponding IR spectra.

2. Materials and methods

2.1. Computational details

2.1.1. Models' nomenclature and binding enthalpy definition. The monomeric unit of β-cyclodextrin was extracted from the corresponding crystallographic structure.[93] Fig. S1 of the ESI† reports top and side views of β-cyclodextrin, with the hydroxylic carbon atoms highlighted, namely C2, C3, and C6. We have arbitrarily named "Head" and "Tail" the parts of the molecule where the hydroxyl groups are located (C2 and C3 belong to the Head, while C6 to the Tail).

The closed and open conformations are called CD1 and CD2, respectively. It is essential to highlight that there is only one possible conformation for CD1, *i.e.*, with all the hydroxyl groups bound to C6 interacting with each other (Fig. S1c, ESI†), as well as for CD2, with all $-CH_2-OH$ groups pointing toward the outermost part of the molecule.

The binding enthalpy of the complex was calculated according to the following formula:

$$BH = (H_{mel} + H_{CD}) - H_{cplx}, \quad (1)$$

where H_{mel} and H_{CD} are the reference enthalpies (*i.e.*, potential energy + zero-point energy + thermal correction at 298 K) of the most stable MT and CD conformers, respectively, while H_{cplx} is the enthalpy of the MT : β-CD complex.

2.1.2. Semiempirical and force-field calculations: xTB code. Simulations with the xTB code (extended Tight-Binding, v. 6.4.0) were carried out at the GFN2 semiempirical level,[94] as well as with the GFN-FF force-field.[95] The considered systems are very flexible, so the submodule CREST (Conformer-Rotamer Ensemble Sampling Tool)[90] was used to explore their potential energy surface and find the most stable conformers, choosing the default accuracy settings (energy convergence $E_{conv} = 5 \times 10^{-6}$ Hartree, gradient convergence $G_{conv} = 1 \times 10^{-3}$ Hartree × Bohr^{-1}, accuracy for integral cutoffs and SCF criteria = 1.0). The NCI mode, *i.e.*, a conformational exploration with optimum settings for non-covalent interacting complexes, was also applied. To avoid non-physical deformations of CDs and to save computing time, all the atoms belonging to the carbonaceous skeleton of CDs were fixed to their starting positions, thus not including them in the conformational exploration. In detail, only the hydroxyl groups bound to the carbon atoms highlighted in Fig. S1 (ESI†) were free to move, including C_6 so that the hydroxymethyl chains could freely rotate. The structures obtained by CREST in the relative stability range of 6 kcal mol^{-1} were then re-optimized at the GFN2 level with tighter thresholds to increase the accuracy of the calculations, that is energy convergence $E_{conv} = 1 \times 10^{-7}$ Hartree, gradient convergence $G_{conv} = 2 \times 10^{-4}$ Hartree × Bohr^{-1} and accuracy of integrals set to = 0.01.

2.1.3. Density functional calculations: ORCA software. Low-lying energy structures obtained by CREST (*i.e.* within kcal mol^{-1} with respect to the most stable one) were re-optimized with the r^{2}SCAN-3c composite density functional,[96–99] using the ORCA code.[100,101] The tolerance in the total energy for the self-consistent field (SCF) iterative procedure was set to $E_{conv} = 1 \times 10^{-8}$ a.u. (default for geometry optimization). The thresholds on geometry optimizations were arranged to the following values: 1×10^{-8} a.u. on the energy difference from two subsequent steps, 3×10^{-5} and 1×10^{-4} Hartree × Bohr^{-1} on Root Mean Square (RMS) and maximum gradients, and 6×10^{-4} and 1×10^{-3} Bohr on RMS and maximum displacements, respectively. Vibrational frequencies were calculated analytically on CD monomers with three main objectives: (i) to ensure that the structures are minima on the Potential Energy Surface – PES, *i.e.* all real frequencies; (ii) to include thermodynamic corrections to the electronic energy and (iii) to simulate IR spectra. Concerning dimers, frequencies were calculated by means of a reduced mass-weighted Hessian matrix (only on the atoms of MT) as obtained by numerical differentiation of the analytical first derivatives, due to the prohibitive memory consumption of a full analytical frequency calculation.

2.2. Materials

β-Cyclodextrin (β-CD) (M_w = 1134.98 g mol^{-1}) was kindly supplied as a gift by Roquette Frères (Lestrem, France). β-CD was dried in an oven at 70 °C up to constant weight before use to remove any traces of water. Melatonin (MT) ($C_{13}H_{16}N_2O_2$, 99 + %), Alfa Aesar, was purchased from ThermoFisher (Kandel, Germany) GmbH. Acetonitrile (H_3CCN, ≥99.9%, for HPLC-Isocratic grade) was purchased from VWR Chemicals BDH (Milano, Italy). Potassium chloride (KCl, ≥99.5% (AT) and sodium chloride) (NaCl, ACS, ISO, Reag. Ph Eur), were purchased from Sigma-Aldrich (Darmstadt, Germany). Disodium hydrogen phosphate dodecahydrate (Na_2HPO_4*$12H_2O$, 99%) and potassium phosphate monobasic (KH_2PO_4, 98%) were purchased from Italia Carlo Erba S.p.A. *Ortho*-phosphoric acid (H_3PO_4, 84–85%) was purchased from Fluka Chemie GmbH, Switzerland. All chemicals were analytical-grade commercial products and were used as received. Deionized water and water purified by reverse osmosis (MilliQ water, Millipore) with a resistivity above 18.2 MΩ cm^{-1} and dispensed through a 0.22 μm membrane filter were used throughout the study.

2.3. Methods

2.3.1. Preparation of the MT : β-CD inclusion complex. MT : β-CD inclusion complexes were prepared using the Nano Spray Dryer B-90 (Büchi Corporation, Switzerland). This procedure was used as an alternative and a novel approach to

Table 1 Amounts of the reactants to prepare MT : β-CD inclusion complexes with different molar ratios

Molar ratio (MT : β-CD)	m MT (g)	m β-CD (g)	V H_2O (mL)
1 : 1	0.20	1.00	50.00
1 : 2	0.10		
2 : 1	0.41		

efficiently prepare the MT : β-CD inclusion complex, although CD and MT complexes have already been prepared with several different methods.[25] For the preparation of the feed solution, accurately weighed amounts of β-CD and MT, in a defined molar ratio, were dissolved in 50 mL of deionized H_2O. A clear solution was observed using a bath sonicator for 10 minutes at 70 °C. The composition of the feed solution is displayed in Table 1.

Inclusion was carried out for 30 minutes while Nano Spray Dryer B-90 was operated under the following conditions: spray mesh with 4.0 μm, inlet temperature 98 °C, outlet temperature 52 °C, spray flow 160 L min^{-1}, aspirator rate 90% and peristaltic pump 70% (~10 mL min^{-1}). The feed solution was continuously kept at 70 °C using a hotplate stirrer equipped with thermoregulation. The spray-dried powders were collected from the cylindrical particle-collecting electrode covered with aluminum foil. Dried nanoparticles were stored in a plastic container under refrigerated conditions. The spray-dried procedure for the formation of MT : β-CD inclusion complexes is schematically represented in Fig. 1.

2.3.2. Fourier transform infrared spectroscopy analysis. Inclusion complexes were characterized through Fourier Transform Infrared Spectroscopy (FTIR) using a PerkinElmer Spectrum Spotlight 100 FTIR spectrophotometer equipped with Spectrum software. FTIR spectra were registered in the spectral range of 4000–650 cm^{-1} with a spectral resolution of 4 cm^{-1} and 16 scans for each sample/background. FTIR spectra were obtained using a versatile Attenuated Total Reflectance mode (FTIR-ATR) sampling accessory with a diamond crystal plate. FTIR-ATR measurements were performed on dried powder samples.

2.3.3. Thermogravimetric analysis. Thermal stability of MT : β-CD inclusion complexes was studied by thermogravimetric analysis (TGA), employing a TA Instrument Thermogravimetric Analyzer Q500 from room temperature up to 700 °C, under nitrogen (N_2) flow, and with a heating ramp rate of 10 °C min^{-1}. The gas flows applied in the balance and furnace sections were 40 mL min^{-1} and 60 mL min^{-1}, respectively. About 10 mg of the sample was weighed in an alumina pan for analysis.

2.3.4. Differential scanning calorimetry. Differential Scanning Calorimetry (DSC) measurements were carried out using a TA instrument Q200 DSC (New Castle, DE, USA) on a 5–6 mg sample under a nitrogen flow of 50 mL min^{-1}. Hermetic aluminum pans were used for the analysis and an empty aluminum pan was used as a reference standard. A heating ramp of 10 °C min^{-1} was applied in the temperature range of 20–180 °C. Each sample was preliminarily dried in an oven at 70 °C for 15 minutes, to eliminate humidity and thus obtain a cleaner signal.

2.3.5. *In vitro* release. MT-release profiles were evaluated using a phosphate-buffered solution (PBS) as a receiving phase with the following formulation: 8 g of NaCl, 0.2 g of KCl, 3.63 g of $Na_2HPO_4 \cdot H_2O$, and 0.24 g of KH_2PO_4 were dissolved in 1 L of deionized H_2O with a pH of 7.4. *In vitro* release tests of MT from MT : β-CD inclusion complexes were performed using the dry powder samples, fixed on an aluminum foil disc, on static vertical Franz Diffusion Cells (PermeGear, Hellertown, PA, USA). Franz Cells were constituted by an upper donor and a lower receptor compartment (volume 12 mL) that were separated by a dialysis tubing cellulose membrane with a contact surface of 1 cm^3, thickness of 45 μm and average flat width of 25 mm. The membrane was immersed overnight in PBS. The sample was placed on top of the membrane in the donor compartment and its amount was varied in a 0.4–0.6 mg range of weight. The receptor compartment was filled with 8 mL of PBS, maintained at 37 °C by a heating jacket under constant stirring (500 rpm). At fixed intervals (30 min, 1 h, 2 h, 3 h, 4 h, 5 h, 6 h) the entire volume of the receptor solution (8 mL) was replaced with the same volume of fresh PBS. Each collected release was filtered through a membrane filter (0.2 μm polytetrafluoroethylene (PTFE), Millipore 13 mm Syringe Filter), and the amount of the released drug was quantified with High-Performance Liquid Chromatography (HPLC-UV). A calibration curve of MT as a standard λ = 223 nm was obtained (R^2 = 0.9994). *In vitro* release tests were performed in triplicate.

2.3.6. High-performance liquid chromatography analysis. High-Performance Liquid Chromatography (HPLC) analysis was carried out at room temperature using a Dionex Acclaim 120 C18 chromatographic column (150 mm × 4.6 mm, particle size 5 μm, pore size 120 Å) connected to a PerkinElmer HPLC system, comprising a Flexar pump working at a flow rate of 1 mL min^{-1} and a Flexar UV-Vis detector set at 223 nm (λ_{max} of MT). The mobile phase was prepared by mixing deionized water (H_2O) and acetonitrile (ACN) with a volume ratio of H_2O:ACN 70 : 30 *v:v*, at a pH = 3 adjusted with H_3PO_4 84–85%. Elution was isocratic and the total run time was set to 6 minutes, while the retention time of melatonin was observed at 5 minutes.

3. Results and discussion

3.1. Conformational exploration of MT : β-CD complex

3.1.1. Melatonin. The planar conformation of the structure of melatonin is depicted in Fig. 2, highlighting the main parts in different colour codes. The molecule is composed of a rigid planar moiety (the indole ring, violet colour in Fig. 2), a methoxy chain (cyan colour), and an amide chain that is free to move around the indole ring (yellow colour). The most stable structure of melatonin in the gas phase is shown in Fig. 3, while the ranking within 4 kcal mol^{-1} of the most stable structures is reported in Table 2. The structures were taken from the existing literature[89,102] and the results were updated with the actual methodology. In the ground state structure, the lateral chain is

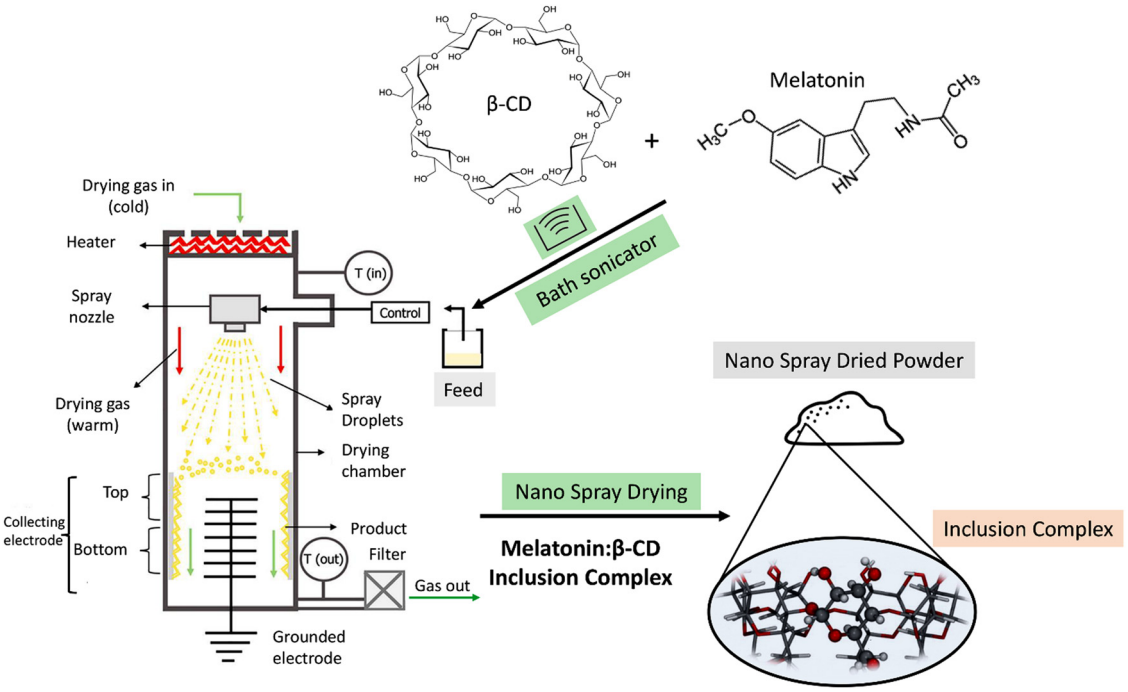

Fig. 1 Schematic representation of the preparation of MT : β-CD inclusion complexes using Nano Spray Dryer B-90.

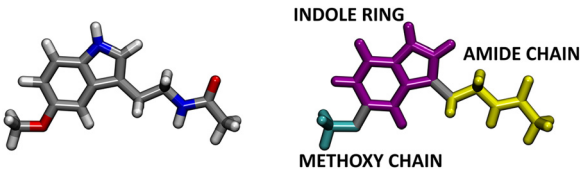

Fig. 2 Licorice representation of the MT molecule in its planar conformation with its atoms (left) and functional groups (right) colour coded. H in white, C in grey, N in blue, O in red.

folded below the ring, to maximize dispersive interactions (see Fig. 3). The r^{2}SCAN-3c results are in good accordance with the golden standard CCSD(T) already presented in the literature, which is an indication that the recently developed composite methods are very accurate for these systems.

3.1.2. MT : β-CD complex. The starting structures of the MT : β-CD complexes were built using the graphical software Moldraw[103] by manually docking the MT molecule in the CD cavity, forming a host–guest complex. MT was inserted in the cavity with two different orientations, due to the non-symmetric structure of both the host and guest molecules, thus forming two different couples of interactions (Metoxy^{MT}-Head^{CD}/Amide^{MT}-Tail^{CD} and Metoxy^{MT}-Tail^{CD}/Amide^{MT}-Head^{CD}, as presented in Fig. S2, ESI†).

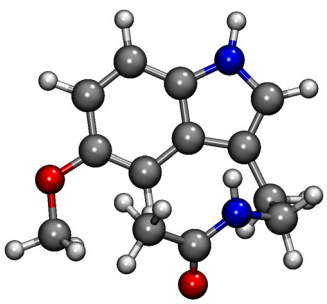

Fig. 3 r^{2}SCAN-3c most stable structure of MT in the gas phase. Atoms colour code: H in white, C in grey, N in blue, and O in red.

Table 2 r^{2}SCAN-3c relative energies (ΔE) of MT conformers in the gas phase. Labels xmm refer to the CREST ranking. Energies are in kcal mol^{-1}

Gas	
Structures	ΔE
x00	0.00
x01	0.83
x03	1.40
x02	1.73
x04	2.09
x15	2.36
x05	2.37
x10	2.70
x11	2.70
x07	2.71
x09	2.88
x06	2.90
x18	3.61
x21	3.63

CD1, as already stated, is the most stable gas phase conformer, so it has certainly to be considered as a host for the gas phase complex, but also CD2 is a good candidate as it presents a wider cavity and, accordingly, is more suitable to form inclusion complexes. The same procedure was applied for both CD1 and CD2, thus generating four input structures for

the CREST program, aiming at expanding, as much as possible, the conformational exploration performed by the automatic CREST tool. Due to the constraints applied to the conformational exploration, the structures obtained by the CREST procedure have also been fully optimized at the GFN2 level and the optimized conformers, characterized by a relative energy below 2 kcal mol^{-1} with respect to the most stable structure, have been reoptimized with r^{2}SCAN-3c.

The CREST conformational search found 73 conformers within the 2 kcal mol^{-1} range, several of which collapsed to the same minimum as a result of the GFN2 optimization. To remove those redundant conformers, the RMSD on the atomic positions of heavy atoms (carbon, oxygen and nitrogen) was run on all the structures with $\Delta E \leq 0.05$ kcal mol^{-1}. Then, if the RMSD value is below 0.125 Å, the structure is considered redundant and deleted (the energy and RMSD thresholds are the same as those of CREST). As a consequence of this check, almost only one-third of the starting 73 structures were reoptimized at the r^{2}SCAN-3c level, avoiding a waste of computational resources.

The r^{2}SCAN-3c most stable structure is shown in Fig. 4, while the binding energy distribution of all the complexes is represented in Fig. 5 as a bar chart. A finer analysis of the binding energy distribution (see Fig. S3, ESI†) points out that the two types of CDs, CD1 and CD2, have a unimodal distribution of BE, centered at higher values for the CD2-type (27 kcal mol^{-1}). Despite the starting geometry of the most stable complex being of the CD2-type, the CREST procedure has moved the hydroxymethyl groups towards the CD innermost part, promoting their interaction either with each other or with melatonin. Therefore, a CD1-type is not properly formed, but the Tail part of the CD has been closed in any case. This justifies the choice of also using CD2 to perform the conformational exploration, as it presents a more suitable cavity to host molecules, that can then close after the complexation reaction has occurred.

3.1.3. MT : β-CD dimer complex. As already pointed out by several experimental studies[16,17,23,104–112] CD can form 1 : 2, 2 : 1, and 2 : 2 complexes, depending on the size of the considered drug. Melatonin is a relatively large molecule, and, accordingly, it is unlikely that a dimer of melatonin enters the CD cavity, as will be discussed in the experimental results

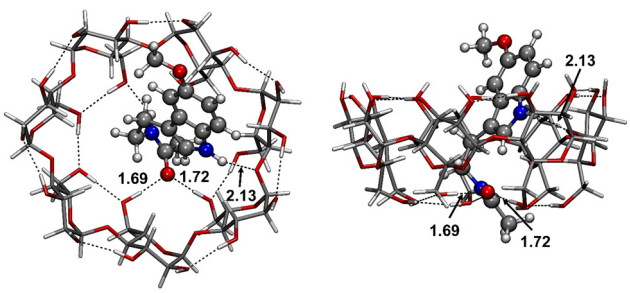

Fig. 4 r^{2}SCAN-3c most stable MT : β-CD complex in the gas phase (left: top view, right: side view). Intermolecular H-bond lengths are reported in Å. Atoms color code: H in white, C in grey, N in blue, and O in red.

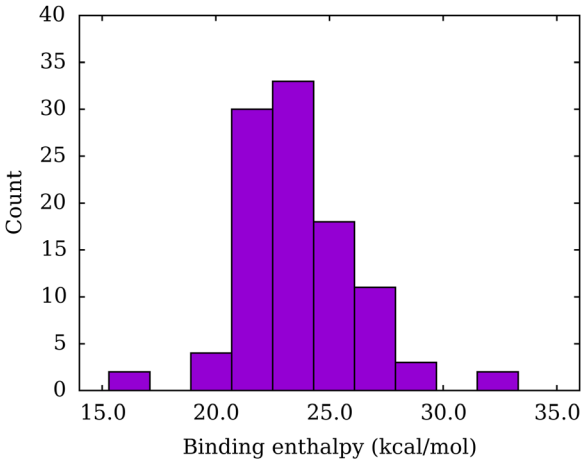

Fig. 5 r^{2}SCAN-3c binding enthalpy (kcal mol^{-1}) distribution for all the MT : β-CD complex structures in the gas phase refined at the DFT level.

section. On the contrary, two molecules of CD are able to complex a single melatonin molecule. This kind of complex is important to be characterized because β-CD can form aggregates due to its low solubility. The most appropriate models to simulate these cases are represented by CD dimers. Indeed, in a previous work, some of us have shown that the formation of CD dimers is thermodynamically favoured, with dimerization energies spanning from −65 to −35 kcal mol^{-1} in the gas phase and from −45 to −37 kcal mol^{-1} in implicit water solvent, depending on the CD conformer used.[41] From a geometric point of view, the length of CD dimers is similar to the length of melatonin (∼13 Å for the β-CD dimer, ∼11 Å for melatonin in its pseudo-planar conformation), allowing for a complete encapsulation of the guest molecule. To evaluate the gas phase ground state, three 1 : 2 complexes were built using β-CD1-HH, β-CD2-HH and β-CD2-TT (labels H and T refer to the H-bond pattern created when dimers are merged from the Head or the Tail part of the CD, see Fig. S1 and S4, ESI†). β-CD1-TT was not considered as it does not have enough space to host melatonin, because of the lack of an open cavity inside the structure (see Fig. S4, ESI†). β-CD1-HH, on the other side, was chosen because it is the most stable dimer in the gas phase, even if the closed conformation of the C6 hydroxyl groups renders the melatonin inclusion very hard. However, we also considered this conformer because it is possible that, after the complexation by β-CD2-HH, the structure may turn to β-CD1-HH, given the flexibility of such a system. In particular, the experimental technique used to prepare the complexes, *i.e.*, Nano Spray Dryer, implies moving from the water solution, where the complexation occurs (and the most stable dimer is β-CD2-HH), to a dry environment. β-CD2-HH and β-CD2-TT were employed because they have a wide cavity, due to their tubular shape, which allows the entrance of melatonin. They are indeed both the most suitable conformers to form these complexes and the most stable structures in the water environment.

Table 3 reports the binding enthalpies of the obtained structures, while Fig. 6 shows the most stable complex in the gas phase; unfortunately, the few conformers found by CREST have not allowed us to build up a reliable bar diagram

Table 3 r²SCAN-3c binding enthalpies (BH) of MT : β-CD dimer complexes. The superscripts indicate the starting CD dimer used to build each complex. Energies are in kcal mol^{-1}

Gas	
Structures	BH
x04$^{\beta\text{-CD1-HH}}$	26.48
x00$^{\beta\text{-CD1-HH}}$	24.96
x27$^{\beta\text{-CD2-HH}}$	15.86
x14$^{\beta\text{-CD2-HH}}$	15.43
x21$^{\beta\text{-CD2-HH}}$	15.19
x20$^{\beta\text{-CD2-HH}}$	14.98
x23$^{\beta\text{-CD2-HH}}$	11.51

distribution of binding energies. According to r²SCAN-3c, the two most stable structures (x04$^{\beta\text{-CD1-HH}}$ and x00$^{\beta\text{-CD1-HH}}$) share the same starting CD dimer, and the complexed structures present the maximum number possible for the H-bond interactions (BH = 26.5 and 25.0 kcal mol^{-1}). On the contrary, if the β-CD2-HH dimer is adopted, not all the H-bonds are formed in the Tail part of the cyclodextrin, thus explaining the lower BH (<16 kcal mol^{-1}).

3.2. Experimental characterizations of MT : βCD inclusion complex

3.2.1. Thermogravimetric analysis (TGA). Thermogravimetric analysis is an effective technique that can be used to evaluate the thermal stability and behaviour of the considered sample. As highlighted in Fig. 7, β-CD presents a degradation step at 340 °C (starting the degradation at 290 °C, highlighted by the orange star), while MT degradation step is at a lower temperature (230 °C, highlighted by the red star). As a consequence, the presence of MT in the inclusion complex slightly reduces the starting degradation temperature to 260 °C, 228 °C and 230 °C for MT : β-CD 1 : 2, MT : β-CD 2 : 1 and MT : β-CD 1 : 1, respectively. A reduction in the TG curves of the complex is possible due to the lower thermal stability of MT, which presents a single degradation step starting at 220 °C. Despite that, the TG losses of MT : β-CD 1 : 1 and MT : β-CD 1 : 2 are very homogeneous along the entire experiment with a single step indicating the mass loss, thus suggesting the formation of

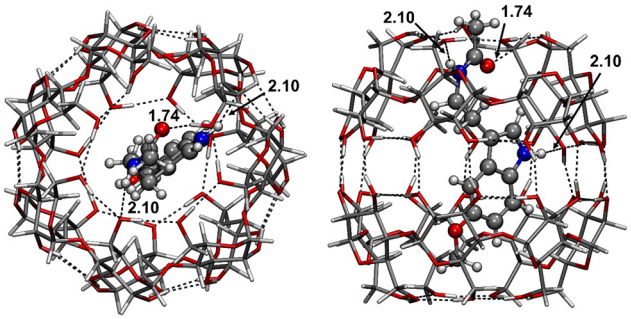

Fig. 6 r²SCAN-3c most stable MT : β-CD dimer complexes in the gas phase. Intermolecular H-bond lengths are reported in Å. The binding enthalpies in parenthesis are in kcal mol^{-1}. Atoms color code: H in white, C in grey, N in blue, and O in red.

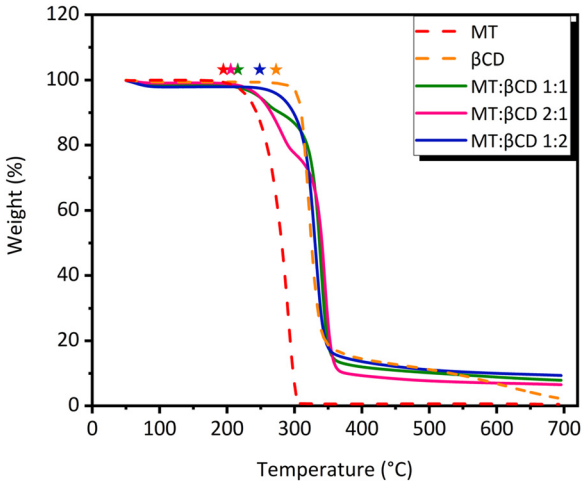

Fig. 7 Thermogravimetric analysis (TGA) of the prepared inclusion complexes compared with the pure β-CD and MT curves.

inclusion complexes. On the contrary, the TGA curve of MT : β-CD 2 : 1 presents two degradation steps, the former being very similar to the bare MT degradation curve, possibly suggesting the formation of MT aggregates along with the MT : β-CD 1 : 1 complex. Such observations suggest that the MT : β-CD 2 : 1 complex is actually a 1 : 1 complex in which the excess of melatonin forms some aggregates.

3.2.2. Differential scanning calorimetry (DSC). Fig. 8 shows the DSC curves of each sample (molar ratio MT : β-CD 1 : 1, MT : β-CD 2 : 1 and MT : β-CD 1 : 2) compared to the respective physical mixture prepared with the corresponding molar ratios of reagents. Physical mixtures are obtained by mixing the dry powders directly in a mortar. DSC thermograms of all physical mixtures (in red) show a characteristic endothermic peak at 118 °C for each sample, which corresponds to the melting point of MT (Fig. 8a). The same peak, however, was not found for DSC curves of inclusion complexes: as highlighted by the blue lines, the curve of inclusion complex MT : β-CD 1 : 1 (Fig. 8b) appears completely flat in the zone between 110 and 120 °C. The lack of the endothermic melatonin melting peak confirms the formation of a host–guest inclusion complex. The same remarks can be extended to the DSC curve of MT : β-CD 1 : 2 (Fig. 8d), although there is a large endothermic signal attributable to the humidity and therefore to the evaporation of water from the sample. In the case of MT : β-CD 2 : 1 (Fig. 8c) a small peak signal at 118 °C can be detected in the sample curve, to suggest the presence of a certain amount of non-complexed MT, which is in line with the findings by TGA. The DSC technique thus confirms the inclusion of MT inside the cavity of β-CD for the complex with 1 : 1 and 2 : 1 molar ratios, resulting in an encapsulation of the drug, thanks to the quick evaporation of the solvent.

3.2.3. *In vitro* releases. The release profiles of MT from the dried powder fixed on an aluminium foil disc, using a Vertical Franz Diffusion Cell, are shown in Fig. 9. The profiles of all three types of the obtained inclusion complexes show a marked tendency to release MT in the very first stage of measurement.

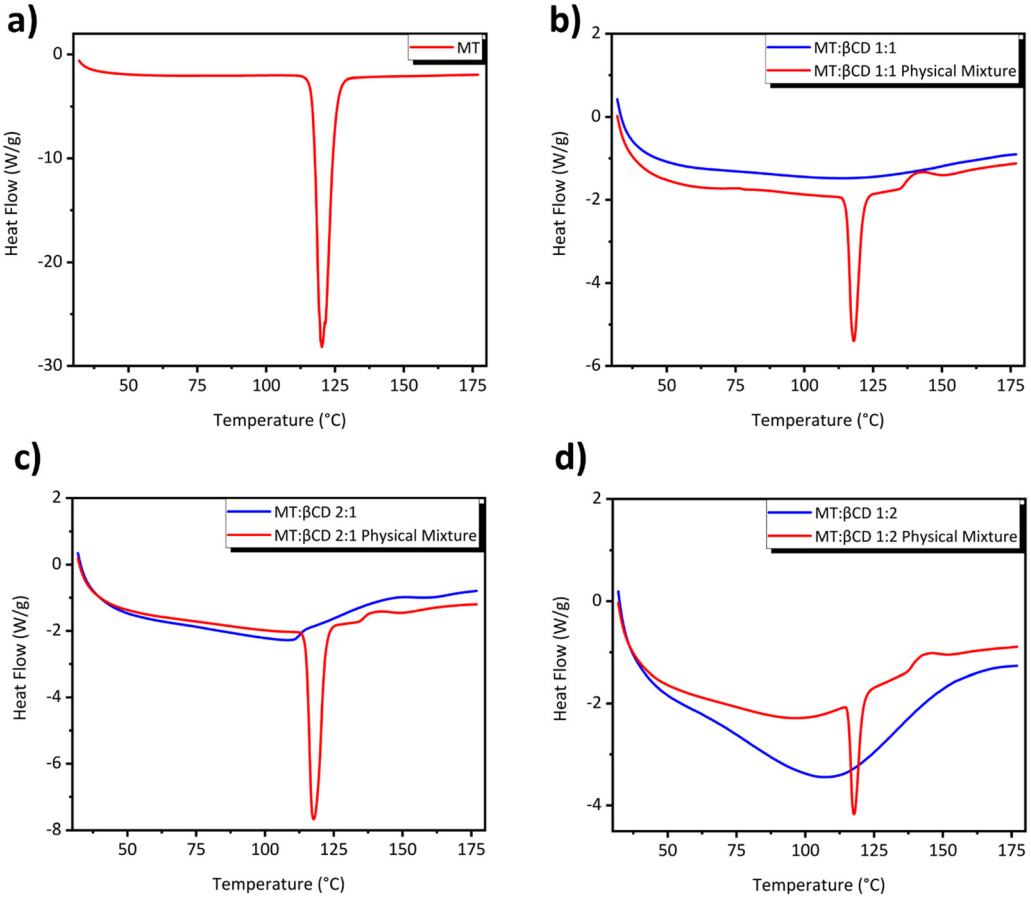

Fig. 8 Differential scanning calorimetry (DSC) thermograms of (a) pure MT, (b) MT : β-CD 1 : 1, (c) MT : β-CD 2 : 1, and (d) MT : β-CD 1 : 2 (blue curves) and corresponding physical mixtures (red curves).

MT : β-CD 2 : 1 sample resulted in the release of 47% of MT. This was associated with the doubled ratio of MT inserted during the preparation, therefore, at 1 hour the released drug reached the plateau. A similar result can be observed for the MT : β-CD 1 : 1 sample with the total quantity of released MT, which does not exceed 48%. In this case, however, the curve shows a smoother profile and does not clearly reach the plateau, featuring a stronger host–guest interaction. Similarly, MT : β-CD, 1 : 2, presents a modulated release rate over time: the percentage of released MT is 33% at 30 min and 43% at 1 h, followed by a constant increase up to 55% after 6 hours. This means that the 1 : 2 complex is a weaker complex than the 1 : 1 one because it releases MT more efficiently than the 1 : 1 complex and in a larger overall amount.

These findings are confirmed by simulations. Indeed, from the computed binding energies, the 1 : 1 complex presents a stronger binding energy (15 to 33 kcal mol^{-1}) with respect to the 2 : 1 (11 to 26 kcal mol^{-1}). This can be ascribed to the fact that in the 1 : 1 complex, the MT-CD interactions are maximized, while in the case of the 1 : 2 complex, they compete with the CD-CD interaction to form the CD dimer.

Fig. S6 of the ESI† shows the actual amount in terms of the mg of MT released by each sample. Since all the inclusion complexes release a similar percentage of MT, results are normalized by the quantity of MT inserted during the preparation of the corresponding inclusion complex, thus showing the released MT in mg of the same quantity of each sample.

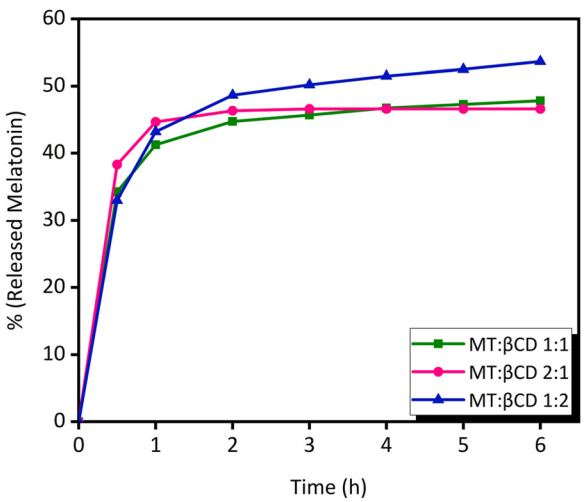

Fig. 9 *In vitro* release profiles of MT from inclusion complexes in the percentage of drug released with respect to the inserted amount in each sample.

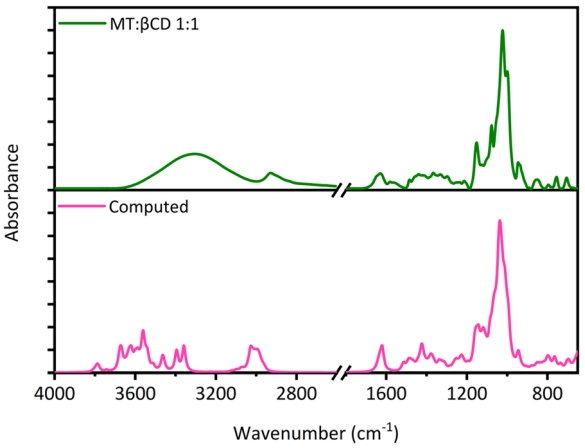

Fig. 10 FTIR experimental (green) and computed (magenta) spectra of the MT : β-CD 1 : 1 inclusion complex.

3.3. FTIR spectroscopy: computed *vs.* experimental

A comparison between computed and experimental IR spectra gives an indication of the accordance between structural models and computational approach, evaluating the similarity of the computed IR spectrum with the experimental one of the MT : β-CD inclusion complex obtained in our laboratory (see Fig. 10). The computed spectrum was collected among all the conformers explored, thus obtaining a more experimentally sound IR spectrum; specifically, the intensities of each single spectrum were scaled by the proper Boltzmann factor, calculated with respect to the most stable structure. Among all the MT : β-CD complex conformers, only the first two stable structures have a non-negligible contribution to the spectrum.

The spectral range comprised between 3600 and 3200 cm^{-1} covers all the possible N–H and O–H stretching modes. For MT, the two N–H groups appear in a band at around 3280 cm^{-1}, attributable to the amide and indole groups. β-CD has a large number of O–H groups in its structure, resulting in a very broad band at 3300 cm^{-1}. The experimental spectrum of the inclusion complex shows the same broad band that dominates and covers any other signals of MT. C–H stretching (aliphatic and aromatic for MT, only aliphatic for β-CD) is in the 3100–2800 cm^{-1} range. The simulated spectrum is blue-shifted with respect to the experimental one of about 150 cm^{-1} because the X—H stretching is strongly affected by anharmonicity, which is too expensive to be included in the frequency calculations. CO moiety of the MT amide group is distinguished at 1618 cm^{-1}, a region completely free of signals for bare β-CD. Consequently, the analysis of the carbonyl peak assumes particular relevance on the inclusion complexes spectra: indeed, all MT : β-CD complexes present a clear signal at the same wavenumber of the MT amide group (1620 cm^{-1}) as direct evidence for the formation of the inclusion complex. For the MT : β-CD 2 : 1 molar ratio, the same peak appears with enhanced intensity and a sharp shape, as a result of the doubled molar ratio of MT and probably of the not complete complexation of MT (see Fig. S5, ESI†). Stretching of aromatic C=C (at around 1600–1500 cm^{-1}), only present in MT, is completely covered by β-CD upon complexation (HCH bending of β-CD appears at 1500–1400 cm^{-1}), and, accordingly, it does not give specific information about the occurrence of complexation or not. The fingerprint area, especially in the range from 1200 to 600 cm^{-1}, appears once again dominated by intense signals of C–O stretching located from β-CD at 1020 cm^{-1}, a typical value for secondary alcohol moieties. The above-mentioned region of the spectrum, *i.e.*, from 1700 cm^{-1} to the fingerprint, is very well reproduced by the computed spectrum, whereas the anharmonic contribution in this case is negligible. Finally, it is worth mentioning, as an added value of the calculations, the good match between the experimental and computed relative intensities, which is usually a quite complex task in simulated spectra.

4. Conclusion

In the present work, we proposed a hybrid approach to formulate and describe the inclusion complex established between MT and β-CD. Experimentally, we prepared the supramolecular cluster with the innovative Nano-Spray Dryer B-90 which allowed us to minimize preparation time and waste of products. Characterizations performed with thermal analyses and FTIR were used to confirm the successful encapsulation of MT inside the β-CD cavity, while *in vitro* studies showed the releases of the MT over time. The molar ratios between MT and β-CD considered in the formulation phase were 1 : 1, 1 : 2 and 2 : 1 and the subsequent characterizations determined the complexation of MT only for the two former molar ratios. In addition, thermal analyses and FTIR on MT : β-CD 2 : 1 showed a non-complete encapsulation of the guest, due to the higher amount of drug with respect to the captivating ability of CD. On the other hand, the CREST algorithm was applied to explore the potential energy surface of the 1 : 1 and 1 : 2 systems, whereas the low-lying conformers were then optimized with the recently released r^2SCAN-3c and vibrational frequencies were calculated with the above method. Results have demonstrated that the stabilization of MT : β-CD 1 : 1 and 1 : 2 complexes is due to non-covalent interactions, mainly H-bonds and dispersive forces. The binding enthalpy distributions show larger binding values for the 1 : 1 complex than the 1 : 2 complex, which was also confirmed by the different MT release profiles from the experimental data. Furthermore, the computed IR spectrum of the MT : β-CD complex is in good agreement with the experimental spectroscopic result, validating the reliability of the model.

Conflicts of interest

There are no conflicts to declare.

Acknowledgements

Authors acknowledge support from Project CH4.0 under the MUR program "Dipartimenti di Eccellenza 2023–2027" (CUP: D13C22003520001). This work has been partially supported by the Spoke 7 "Materials and Molecular Sciences" of ICSC –

Centro Nazionale di Ricerca in High-Performance Computing, Big Data and Quantum Computing, funded by the European Union – NextGenerationEU. We kindly acknowledge Roquette Frères (Lestrem, France), for providing the β-cyclodextrin (β-CD) and Piero Ugliengo (Department of Chemistry of the University of Turin, Italy), for fruitful discussion. R. F. is indebted to MUR for his PhD grant PON DM1061. The research activity of G. H. is part of the project NODES which has received funding from the MUR–M4C2 1.5 of PNRR with the grant agreement no. ECS00000036. We acknowledge the CINECA award under the ISCRA initiative, for the availability of high performance computing resources and support.

References

1 J. Cipolla-Neto and F. G. Do Amaral, Melatonin as a Hormone: New Physiological and Clinical Insights, *Endocr. Rev.*, 2018, **39**(6), 990–1028.
2 V. Srinivasan, D. W. Spence, S. R. Pandi-Perumal, I. Trakht and D. P. Cardinali, Jet lag: Therapeutic use of melatonin and possible application of melatonin analogs, *Travel Med. Infect. Dis.*, 2008, **6**(1–2), 17–28.
3 J. Z. Nowak and J. B. Zawilska, Melatonin and its physiological and therapeutic properties, *Pharm. World Sci.*, 1998, **20**, 18–27.
4 S. R. Pandi-Perumal, N. Zisapel, V. Srinivasan and D. P. Cardinali, Melatonin and sleep in aging population, *Exp. Gerontol.*, 2005, **40**(12), 911–925.
5 A. Chrustek and D. Olszewska-Słonina, Melatonin as a powerful antioxidant, *Acta Pharm.*, 2021, **71**, 335–354.
6 C. del Valle Bessone, H. D. Fajreldines, G. E. D. de Barboza, N. G. Tolosa de Talamoni, D. A. Allemandi, A. R. Carpentieri and D. A. Quinteros, Protective role of melatonin on retinal ganglionar cell: In vitro an in vivo evidences, *Life Sci.*, 2019, **218**, 233–240.
7 S. Tengattini, R. J. Reiter, D. X. Tan, M. P. Terron, L. F. Rodella and R. Rezzani, Cardiovascular diseases: protective effects of melatonin, *J. Pineal Res.*, 2008, **44**(1), 16–25.
8 M. Imenshahidi, G. Karimi and H. Hosseinzadeh, Effects of melatonin on cardiovascular risk factors and metabolic syndrome: a comprehensive review, *Naunyn-Schmiedeberg's Arch. Pharmacol.*, 2020, **393**, 521–536.
9 A. Romero, J. Morales-García and E. Ramos, Melatonin: a multitasking indoleamine to modulate hippocampal neurogenesis, *Neural Regener. Res.*, 2023, **18**(3), 503–505.
10 A. Hafner, J. Lovrić, D. Voinovich and J. Filipović-Grčić, Melatonin-loaded lecithin/chitosan nanoparticles: Physicochemical characterisation and permeability through Caco-2 cell monolayers, *Int. J. Pharm.*, 2009, **381**(2), 205–213.
11 L. Bénès, B. Claustrat, F. Horrière, M. Geoffriau, J. Konsil, K. A. Parrott, G. Degrande, R. L. Mcquinn and J. W. Ayres, Transmucosal, Oral Controlled-Release, and Transdermal Drug Administration in Human Subjects: A Crossover Study with Melatonin, *J. Pharm. Sci.*, 1997, **86**(10), 1115–1119.
12 Y. Li, X. Zhao, Y. Zu, L. Wang, W. Wu, Y. Deng, C. Zu and Y. Liu, Melatonin-loaded silica coated with hydroxypropyl methylcellulose phthalate for enhanced oral bioavailability: Preparation, and in vitro-in vivo evaluation, *Eur. J. Pharm. Biopharm.*, 2017, **112**, 58–66.
13 A. Zafra-Roldán, S. Corona-Avendaño, R. Montes-Sánchez, M. Palomar-Pardavé, M. Romero-Romo and M. T. Ramírez-Silva, New insights on the spectrophotometric determination of melatonin pKa values and melatonin-βCD inclusion complex formation constant, *Spectrochim. Acta, Part A*, 2018, **190**, 442–449.
14 A. M. Khattabi, W. H. Talib and D. A. Alqdeimat, A targeted drug delivery system of anti-cancer agents based on folic acid-cyclodextrin-long polymer functionalized silica nanoparticles, *J. Drug Delivery Sci. Technol.*, 2017, **41**, 367–374.
15 J. Łagiewka, T. Girek and W. Ciesielski, Cyclodextrins-Peptides/Proteins Conjugates: Synthesis, Properties and Applications, *Polymers*, 2021, **13**, 1759.
16 R. Periasamy, Cyclodextrin-based molecules as hosts in the formation of supramolecular complexes and their practical applications—A review, *J. Carbohydr. Chem.*, 2021, **40**(4), 135–155.
17 D. Bongiorno, L. Ceraulo, M. Ferrugia, F. Filizzola, A. Ruggirello and V. T. Liveri, Inclusion complexes of cyclomaltooligosaccharides (cyclodextrins) with melatonin in solid phase, *ARKIVOC*, 2005, 118–130.
18 M. Vlachou, M. Papamichael, A. Siamidi, I. Fragouli, P. A. Afroudakis, R. Kompogennitaki and Y. Dotsikas, Comparative In Vitro Controlled Release Studies on the Chronobiotic Hormone Melatonin from Cyclodextrins-Containing Matrices and Cyclodextrin: Melatonin Complexes, *Int. J. Mol. Sci.*, 2017, **18**(8), 1641.
19 G. Hoti, R. Ferrero, F. Caldera, F. Trotta, M. Corno, S. Pantaleone, M. M. H. Desoky and V. Brunella, A Comparison between the Molecularly Imprinted and Non-Molecularly Imprinted Cyclodextrin-Based Nanosponges for the Transdermal Delivery of Melatonin, *Polymers*, 2023, **15**, 1543.
20 E. M. M. Del Valle, Cyclodextrins and their uses: a review, *Process Biochem.*, 2004, **39**(9), 1033–1046.
21 P. Jansook, N. Ogawa and T. Loftsson, Cyclodextrins: structure, physicochemical properties and pharmaceutical applications, *Int. J. Pharm.*, 2018, **535**(1–2), 272–284.
22 S. S. Jambhekar and P. Breen, Cyclodextrins in pharmaceutical formulations I: structure and physicochemical properties, formation of complexes, and types of complex, *Drug Discovery Today*, 2016, **21**(2), 356–362.
23 H. Dodziuk, *Cyclodextrins and Their Complexes: Chemistry, Analytical Methods, Applications*, John Wiley and Sons, 2006.
24 K. Uekama, F. Hirayama and T. Irie, Cyclodextrin Drug Carrier Systems, *Chem. Rev.*, 1998, **98**(5), 2045–2076.
25 A. Sakellaropoulou, A. Siamidi and M. Vlachou, Melatonin/Cyclodextrin Inclusion Complexes: A Review, *Molecules*, 2022, **27**(2), 445.
26 G. B. Celli, A. Ghanem and M. S. L. Brooks, Bioactive Encapsulated Powders for Functional Foods—a Review of

Methods and Current Limitations, *Food Bioprocess Technol.*, 2015, **8**, 1825–1837.
27 C. Arpagaus, A. Collenberg, D. Rütti, E. Assadpour and S. M. Jafari, Nano spray drying for encapsulation of pharmaceuticals, *Int. J. Pharm.*, 2018, **546**(1–2), 194–214.
28 A. Gharsallaoui, G. Roudaut, O. Chambin, A. Voilley and R. Saurel, Applications of spray-drying in microencapsulation of food ingredients: An overview, *Food Res. Int.*, 2007, **40**(9), 1107–1121.
29 M. Saifullah, M. R. I. Shishir, R. Ferdowsi, M. R. Tanver Rahman and Q. Van Vuong, Micro and nano encapsulation, retention and controlled release of flavor and aroma compounds: A critical review, *Trends Food Sci. Technol.*, 2019, **86**, 230–251.
30 M. Mirankó, M. Megyesi, Z. Miskolczy, J. Tóth, T. Feczkó and L. Biczók, Encapsulation of Metronidazole in Biocompatible Macrocycles and Structural Characterization of Its Nano Spray-Dried Nanostructured Composite, *Molecules*, 2021, **26**(33), 7335.
31 V. Lavelli and J. Sereikaitė, Kinetic Study of Encapsulated β-Carotene Degradation in Dried Systems: A Review, *Foods*, 2021, **11**(3), 437.
32 R. Silva-Carvalho, J. Fidalgo, K. R. Melo, M. F. Queiroz, S. Leal, H. A. Rocha, T. Cruz, P. Parpot, A. M. Tomás and M. Gama, Development of dextrin-amphotericin B formulations for the treatment of Leishmaniasis, *Int. J. Biol. Macromol.*, 2020, **153**, 276–288.
33 H. M. C. Marques, A review on cyclodextrin encapsulation of essential oils and volatiles, *Flavour Fragrance J.*, 2010, **25**(5), 313–326.
34 M. Mirankó, J. Tóth, C. Bartos, R. Ambrus and T. Feczkó, Nano-Spray-Dried Levocetirizine Dihydrochloride with Mucoadhesive Carriers and Cyclodextrins for Nasal Administration, *Pharmaceutics*, 2023, **15**(2), 317.
35 W. Wang, Z. Ye, H. Gao and D. Ouyang, Computational pharmaceutics – A new paradigm of drug delivery, *J. Controlled Release*, 2021, **338**, 119–136.
36 T. Ashwini, R. Narayan, P. A. Shenoy and U. Y. Nayak, Computational modeling for the design and development of nano based drug delivery systems, *J. Mol. Liq.*, 2022, **368**, 120596.
37 A. H. Mazurek, Ł. Szeleszczuk and T. Gubica, Application of Molecular Dynamics Simulations in the Analysis of Cyclodextrin Complexes, *Int. J. Mol. Sci.*, 2021, **22**(17), 9422.
38 A. H. Mazurek and Ł. Szeleszczuk, Current Status of Quantum Chemical Studies of Cyclodextrin Host–Guest Complexes, *Molecules*, 2022, **27**(12), 3874.
39 Y. Belhocine, S. Rahali, H. Allal, I. M. Assaba, M. G. Ghoniem and F. A. M. Ali, A Dispersion Corrected DFT Investigation of the Inclusion Complexation of Dexamethasone with β-Cyclodextrin and Molecular Docking Study of Its Potential Activity against COVID-19, *Molecules*, 2021, **26**(24), 7622.
40 A. Stachowicz, A. Styrcz, J. Korchowiec, A. Modaressi and M. Rogalski, DFT studies of cation binding by β-cyclodextrin, *Theor. Chem. Acc.*, 2011, **130**, 939–953.
41 S. Pantaleone, C. I. Gho, R. Ferrero, V. Brunella and M. Corno, Exploration of the conformational scenario for α-, β-, and γ-cyclodextrins in dry and wet conditions, from monomer to crystal structures: a quantum-mechanical study, *Int. J. Mol. Sci.*, 2023, **24**(23), 16826.
42 X. Bao, X. Liu, R. Dou, S. Xu, D. Liu, J. Luo, X. Gong, C. F. Wong and B. Zhou, How are N-methylcarbamates encapsulated by β-cyclodextrin: insight into the binding mechanism, *Phys. Chem. Chem. Phys.*, 2023, **25**, 13923–13932.
43 T. Aree, Atomic-level understanding on conformational flexibility of neochlorogenic and chlorogenic acids and their inclusion complexation with β-cyclodextrin, *Food Hydrocolloids*, 2023, **141**, 108742.
44 B. Nie, J. Yan, S. Shi, L. J. Wang, Y. C. Wu and H. J. Li, Sustainable corrosion resistance of piroxicam-cyclodextrin inclusion complex to mild steel and its mechanism, *J. Mater. Res. Technol.*, 2023, **23**, 3665–3675.
45 A. S. Al-Jaber and A. D. Bani-Yaseen, On the encapsulation of Olsalazine by β-cyclodextrin: A DFT-based computational and spectroscopic investigations, *Spectrochim. Acta, Part A*, 2019, **214**, 531–536.
46 W. Li, B. Lu, A. Sheng, F. Yang and Z. Wang, Spectroscopic and theoretical study on inclusion complexation of beta-cyclodextrin with permethrin, *J. Mol. Struct.*, 2010, **981**(1–3), 194–203.
47 A. Zaboub, F. Madi, R. Merdes, M. Mohamedi and L. Nouar, A combined DFT and experimental study of proline/β-cyclodextrin inclusion complex, *J. Mol. Liq.*, 2016, **216**, 716–723.
48 M. Nora, L. Ismahan, G. Abdelkrim, C. Mouna, N. Leila, M. Fatiha, B. Nada and H. Brahim, Interactions in inclusion complex of β-cyclodextrin/L-Metheonine: DFT computational studies, *J. Inclusion Phenom. Macrocyclic Chem.*, 2020, **96**, 43–54.
49 P. H. S. Paulino, S. M. R. de Sousa, H. C. Da Silva, W. B. De Almeida, J. L. Ferrari, L. Guimarães and C. S. Nascimento, A theoretical investigation on the encapsulation process of mepivacaine into β-cyclodextrin, *Chem. Phys. Lett.*, 2020, **740**, 137060.
50 H. Bouchemela, F. Madi and L. Nouar, DFT investigation of host–guest interactions between α-Terpineol and β-cyclodextrin, *J. Inclusion Phenom. Macrocyclic Chem.*, 2019, **95**, 247–258.
51 A. Benaïssa, A. Bouhadiba, N. Naili, F. Chekkal, M. Khelfaoui, I. Bouras, M. S. Madjram, B. Zouchoune, S. Mogalli, N. Malfi, L. Nouar and F. Madi, Computational investigation of dimethoate and β-cyclodextrin inclusion complex: molecular structures, intermolecular interactions, and electronic analysis, *Struct. Chem.*, 2023, **34**, 1189–1204.
52 W. Imamura, T. Yamasaki, H. Kato and T. Ishikawa, Insights into the molecular interaction of cyclodextran with a guest molecule: A computational study, *Carbohydr. Polym.*, 2023, **301**, 120315.
53 W. F. da Silva, E. dos Santos Niculau, D. A. B. de Oliveira, M. W. V. de Assis and M. N. Oliveira, Preparation,

physicochemical characterization and computational studies of Plectranthus ornatus codd essential oil/β-cyclodextrin inclusion complex, *J. Mol. Struct.*, 2023, **1285**, 135476.

54 S. Badi, F. Madi, L. Nouar and A. Gheid, Effect of cyclodextrins inclusion complexes into absorption and emission spectra of P-methylaminobenzoate derivatives: A DFT and TD-DFT investigation, *J. Fluoresc.*, 2023, **33**, 1457–1467.

55 J. T. Hołaj-Krzak, Theoretical studies of interactions in cyprodinil–α-cyclodextrin and cyprodinil–β-cyclodextrin systems, *J. Water Land Dev.*, 2023, **57**, 9–20.

56 A. Ferino-Pérez, Q. Portorreal, J. J. Gamboa-Carballo, B. Minofar, S. Gaspard and U. J. Jaúregui-Haza, Competitive formation of molecular inclusion complexes of chlordecone and β-hexachlorocyclohexane with natural cyclodextrins: DFT and molecular dynamics study, *J. Mol. Model.*, 2023, **29**, 196.

57 V. Ganesan, M. K. Mani, V. Narayanan, E. Shanmugasundram, K. Vellaisamy, V. Baskaralingam, J. Jeyaraj, G. B. Veerakanellore, R. Rajamohan and S. Thambusamy, Synthesis, characterization of 4,4′-((1E,1′E)-hydrazine-1,2-diylidenebis(methanylylidene)) diphenol and the inclusion complex with γ-cyclodextrin as a fluorescent probe for detection of Al^{3+}, *J. Photochem. Photobiol., A*, 2023, **442**, 114814.

58 I. Djellala, N. Merabet, L. Nouar, F. Madi, A. Guendouzi and A. Bouhadiba, Host–Guest Inclusion Systems of Vanillic Acid into α-Cyclodextrin: Structures, Electronic Properties, QTAIM, NCI and IGM Analyses with Dispersion Corrected Calculations, *Polycyclic Aromat. Compd.*, 2023, 1–15.

59 S. Benghodbane and D. Khatmi, Quantum chemical calculations based on ONIOM and the DFT methods in the inclusion complex: doxycycline/2-O-Me-β-cyclodextrin, *J. Inclusion Phenom. Macrocyclic Chem.*, 2012, **77**, 231–240.

60 L. E. Afahanam, H. Louis, I. Benjamin, T. E. Gber, I. J. Ikot and A. L. E. Manicum, Heteroatom (B, N, P, and S)-Doped Cyclodextrin as a Hydroxyurea (HU) Drug Nanocarrier: A Computational Approach, *ACS Omega*, 2023, **8**(11), 9861–9872.

61 G. Jafari, H. Raissi, A. Saberinasab and S. Pasban, Phosphatidylcholine in the tear film of the eye: Enhanced topical delivery of fluorometholone to the eye, *Inorg. Chem. Commun.*, 2023, **150**, 110506.

62 M. Khavani, R. Kalantarinezhad and M. Izadyar, A joint QM/MD study on α-, β- and γ-cyclodextrins in selective complexation with cathinone, *Supramol. Chem.*, 2018, **30**, 687–696.

63 E. Christoforides, K. Fourtaka, A. Andreou and K. Bethanis, X-ray crystallography and molecular dynamics studies of the inclusion complexes of geraniol in β-cyclodextrin, heptakis (2,6-di-O-methyl)-β-cyclodextrin and heptakis (2,3,6-tri-O-methyl)-β-cyclodextrin, *J. Mol. Struct.*, 2020, **1202**, 127350.

64 C. Kouderis, S. Tsigoias, P. Siafarika and A. G. Kalampounias, The Effect of Alkali Iodide Salts in the Inclusion Process of Phenolphthalein in β-Cyclodextrin: A Spectroscopic and Theoretical Study, *Molecules*, 2023, **28**(3), 1147.

65 G. Raffaini and F. Ganazzoli, Molecular dynamics study of host–guest interactions in cyclodextrins: methodology and data analysis for a comparison with solution data and the solid-state structure, *J. Inclusion Phenom. Macrocyclic Chem.*, 2007, **57**, 683–688.

66 X. Yao, Molecular dynamics simulation on β-cyclodextrin and steroids, *Acta Chim. Sin.*, 2009, **67**(12), 1318–1324.

67 G. Raffaini, A. Mazzaglia and M. Catauro, Molecular Dynamics Study of Sorafenib Anti-Cancer Drug: Inclusion Complex in Amphiphilic Cyclodextrin, *Macromol. Symp.*, 2021, **395**, 2000201.

68 G. Raffaini and F. Ganazzoli, A Molecular Dynamics Study of the Inclusion Complexes of C60 with Some Cyclodextrins, *J. Phys. Chem. B*, 2010, **114**(21), 7133–7139.

69 P. Wongpituk, B. Nutho, W. Panman, N. Kungwan, P. Wolschann, T. Rungrotmongkol and N. Nunthaboot, Structural dynamics and binding free energy of neral-cyclodextrins inclusion complexes: molecular dynamics simulation, *Mol. Simul.*, 2017, **43**(13–16), 1356–1363.

70 G. Kaniraja, M. Karthikeyan, M. D. Kumar, K. Arunsunai Kumar and C. Karunakaran, Theoretical and electrochemical studies of host-guest inclusion complexes formed between L-Tryptophan with α- and β-cyclodextrins, *J. Mol. Struct.*, 2023, **1291**, 136064.

71 F. Castiglione, F. Ganazzoli, L. Malpezzi, A. Mele, W. Panzeri and G. Raffaini, Inclusion complexes of β-cyclodextrin with tricyclic drugs: an X-ray diffraction, NMR and molecular dynamics study, *Beilstein J. Org. Chem.*, 2017, **13**, 714–719.

72 M. Chen, Y. H. Li, Y. G. Li, X. L. Li, S. Y. Zhao, L. J. Yang, X. Y. Liu and J. Q. Zhang, Molecular dynamics simulations and theoretical calculations of cyclodextrin-polydatin inclusion complexes, *J. Mol. Struct.*, 2021, **1230**, 129840.

73 M. I. Sancho, S. Andujar, R. D. Porasso and R. D. Enriz, Theoretical and Experimental Study of Inclusion Complexes of β-Cyclodextrins with Chalcone and 2′,4′-Dihydroxychalcone, *J. Phys. Chem. B*, 2016, **120**(12), 3000–3011.

74 G. Raffaini and F. Ganazzoli, Understanding Surface Interaction and Inclusion Complexes between Piroxicam and Native or Crosslinked β-Cyclodextrins: The Role of Drug Concentration, *Molecules*, 2020, **25**, 2848.

75 G. Raffaini, S. Elli, F. Ganazzoli and M. Catauro, Inclusion Complexes Between β-cyclodextrin and the Anticancer Drug 5-Fluorouracil for its Solubilization: a Molecular Dynamics Study at Different Stoichiometries, *Macromol. Symp.*, 2022, **404**, 2100305.

76 J. Pozuelo, A. Nakamura and F. Mendicuti, Molecular Mechanics Study of the Complexes of β-Cyclodextrin with 4-(dimethylamino)benzonitrile and Benzonitrile, *J. Inclusion Phenom.*, 1999, **35**, 467–485.

77 M. B. de Jesus, L. de Matos Alves Pinto, L. F. Fraceto, Y. Takahata, A. C. S. Lino, C. Jaime and E. de Paula, Theoretical and experimental study of a praziquantel and

β-cyclodextrin inclusion complex using molecular mechanic calculations and 1H-nuclear magnetic resonance, *J. Pharm. Biomed. Anal.*, 2006, **41**, 1428–1432.

78 M. Cervero and F. Mendicuti, Inclusion Complexes of Dimethyl 2,6-Naphthalenedicarboxylate with α- and β-Cyclodextrins in Aqueous Medium: Thermodynamics and Molecular Mechanics Studies, *J. Phys. Chem. B*, 2000, **104**, 1572–1580.

79 F. Fateminasab, A. K. Bordbar, S. Shityakov and A. A. Saboury, Molecular insights into inclusion complex formation between β- and γ-cyclodextrins and rosmarinic acid, *J. Mol. Liq.*, 2020, **314**, 113802.

80 V. Venuti, V. Crupi, B. Fazio, D. Majolino, G. Acri, B. Testagrossa, R. Stancanelli, F. De Gaetano, A. Gagliardi, D. Paolino, G. Floresta, V. Pistarà, A. Rescifina and C. A. Ventura, Physicochemical characterization and antioxidant activity evaluation of idebenone/hydroxypropyl-β-cyclodextrin inclusion complex, *Biomolecules*, 2019, **9**, 9100531.

81 E. Alvira, Theoretical study of the β-cyclodextrin inclusion complex formation of eugenol in water, *Molecules*, 2018, **23**, 928.

82 B. Nutho, W. Khuntawee, C. Rungnim, P. Pongsawasdi, P. Wolschann, A. Karpfen, N. Kungwan and T. Rungrotmongkol, Binding mode and free energy prediction of fisetin/β-cyclodextrin inclusion complexes, *Beilstein J. Org. Chem.*, 2014, **10**, 2789–2799.

83 S. Grimme, Exploration of Chemical Compound, Conformer, and Reaction Space with Meta-Dynamics Simulations Based on Tight-Binding Quantum Chemical Calculations, *J. Chem. Theory Comput.*, 2019, **15**(5), 2847–2862.

84 J. A. Platts, Quantum chemical molecular dynamics and metadynamics simulation of aluminium binding to amyloid-β and related peptides, *R. Soc. Open Sci.*, 2020, **7**(2), 191562.

85 F. Bohle and S. Grimme, Efficient structural and energetic screening of fullerene encapsulation in a large supramolecular double decker macrocycle, *J. Serb. Chem. Soc.*, 2019, **84**(8), 837–844.

86 D. Serillon, C. Bo and X. Barril, Testing automatic methods to predict free binding energy of host–guest complexes in SAMPL7 challenge, *J. Comput.-Aided Mol. Des.*, 2021, **35**, 209–222.

87 H. Barbero and E. Masson, Design and recognition of cucurbituril-secured platinum-bound oligopeptides, *Chem. Sci.*, 2021, **12**, 9962–9968.

88 C. P. A. Anconi and L. C. A. Souza, Multi-equilibrium approach to study cyclodextrins host–guest systems with GFN2-xTB quantum method: A case study of phosphorothioates included in β-cyclodextrin, *Comput. Theor. Chem.*, 2022, **1217**, 113916.

89 R. Ferrero, S. Pantaleone, M. Delle Piane, F. Caldera, M. Corno, F. Trotta and V. Brunella, Molecules, On the Interactions of Melatonin/β-Cyclodextrin Inclusion Complex: A Novel Approach Combining Efficient Semiempirical Extended Tight-Binding (xTB) Results with Ab Initio Methods, *Molecules*, 2021, **26**(19), 5881.

90 P. Pracht, F. Bohle and S. Grimme, Automated exploration of the low-energy chemical space with fast quantum chemical methods, *Phys. Chem. Chem. Phys.*, 2020, **22**, 7169–7192.

91 S. Spicher, M. Bursch and S. Grimme, Efficient Calculation of Small Molecule Binding in Metal–Organic Frameworks and Porous Organic Cages, *J. Phys. Chem. C*, 2020, **124**(50), 27529–27541.

92 E. Boz and M. Stein, Accurate Receptor-Ligand Binding Free Energies from Fast QM Conformational Chemical Space Sampling, *Int. J. Mol. Sci.*, 2021, **22**(6), 3078.

93 A. I. Ramos, T. M. Braga, P. Silva, J. A. Fernandes, P. Ribeiro-Claro, M. De Fátima Silva Lopes, F. A. A. Paz and S. S. Braga, Chloramphenicol·cyclodextrin inclusion compounds: co-dissolution and mechanochemical preparations and antibacterial action, *CrystEngComm*, 2013, **15**, 2822–2834.

94 C. Bannwarth, S. Ehlert and S. Grimme, GFN2-xTB—An Accurate and Broadly Parametrized Self-Consistent Tight-Binding Quantum Chemical Method with Multipole Electrostatics and Density-Dependent Dispersion Contributions, *J. Chem. Theory Comput.*, 2019, **15**(3), 1652–1671.

95 S. Spicher and S. Grimme, Robust Atomistic Modeling of Materials, Organometallic, and Biochemical Systems, *Angew. Chem.*, 2020, **132**(36), 15795–15803.

96 E. Caldeweyher, S. Ehlert, A. Hansen, H. Neugebauer, S. Spicher, C. Bannwarth and S. Grimme, A generally applicable atomic-charge dependent London dispersion correction, *J. Chem. Phys.*, 2019, **150**(15), 154122.

97 H. Kruse and S. Grimme, A geometrical correction for the inter- and intra-molecular basis set superposition error in Hartree-Fock and density functional theory calculations for large systems, *J. Chem. Phys.*, 2012, **136**(15), 154101.

98 S. Grimme, A. Hansen, S. Ehlert and J. M. Mewes, r^{2}SCAN-3c: A ''Swiss army knife'' composite electronic-structure method, *J. Chem. Phys.*, 2021, **154**(6), 064103.

99 F. Weigend and R. Ahlrichs, Balanced basis sets of split valence, triple zeta valence and quadruple zeta valence quality for H to Rn: Design and assessment of accuracy, *Phys. Chem. Chem. Phys.*, 2005, **7**, 3297–3305.

100 F. Neese, F. Wennmohs, U. Becker and C. Riplinger, The ORCA quantum chemistry program package, *J. Chem. Phys.*, 2020, **152**(22), 224108.

101 F. Neese, The ORCA program system, *Wiley Interdiscip. Rev.: Comput. Mol. Sci.*, 2011, **2**(1), 73–78.

102 U. R. Fogueri, S. Kozuch, A. Karton and J. M. L. Martin, The Melatonin Conformer Space: Benchmark and Assessment of Wave Function and DFT Methods for a Paradigmatic Biological and Pharmacological Molecule, *J. Phys. Chem. A*, 2013, **117**(10), 2269–2277.

103 P. Ugliengo, D. Viterbo and G. Chiari, MOLDRAW: Molecular graphics on a personal computer, *Z. Kristallogr. – Cryst. Mater.*, 1993, **207**, 9–23.

104 I. Matei, A. Nicolae and M. Hillebrand, Fluorimetric and molecular mechanics study of the inclusion complex of 2-quinoxalinyl-phenoxathiin with β-cyclodextrin, *J. Inclusion Phenom. Macrocyclic Chem.*, 2007, **57**, 597–601.

105 P. Lv, D. Zhang, M. Guo, J. Liu, X. Chen, R. Guo, Y. Xu, Q. Zhang, Y. Liu, H. Guo and M. Yang, Structural analysis and cytotoxicity of host-guest inclusion complexes of cannabidiol with three native cyclodextrins, *J. Drug Delivery Sci. Technol.*, 2019, **51**, 337–344.

106 K. Uekama, T. F. ujinaga, F. Hirayama, M. Otagiri and M. Yamasaki, Inclusion complexations of steroid hormones with cyclodextrins in water and in solid phase, *Int. J. Pharm.*, 1982, **10**, 1–15.

107 Z. Aytac, S. I. Kusku, E. Durgun and T. Uyar, Quercetin/β-cyclodextrin inclusion complex embedded nanofibres: Slow release and high solubility, *Food Chem.*, 2016, **197**, 864–871.

108 J. N. Moorthy, K. Venkatesan and R. G. Weiss, Photodimerization of Coumarins in Solid Cyclodextrin Inclusion Complexes, *J. Org. Chem.*, 1992, **57**, 3292–3297.

109 C. Yuan, Z. Jin and X. Xu, Inclusion complex of astaxanthin with hydroxypropyl-β-cyclodextrin: UV, FTIR, 1H NMR and molecular modeling studies, *Carbohydr. Polym.*, 2012, **89**(2), 492–496.

110 A. Mallick, B. Haldar and N. Chattopadhyay, Encapsulation of norharmane in cyclodextrin: formation of 1:1 and 1:2 inclusion complexes, *J. Photochem. Photobiol., B*, 2005, **78**(3), 215–221.

111 J. W. Park and H. J. Song, Association of anionic surfactants with beta-cyclodextrin: fluorescence-probed studies on the 1:1 and 1:2 complexation, *J. Phys. Chem.*, 1989, **93**, 6454–6458.

112 X. Wen, F. Tan, Z. Jing and Z. Liu, Preparation and study the 1:2 inclusion complex of carvedilol with β-cyclodextrin, *J. Pharm. Biomed. Anal.*, 2004, **34**(3), 517–523.